Carbohydrate Polymers 80 (2010) 420–425

Contents lists available at ScienceDirect

Carbohydrate Polymers

journal homepage: www.elsevier.com/locate/carbpol

Starch-based composites reinforced with novel chitin nanoparticles

Peter R. Chang [b,c,*], Ruijuan Jian [a], Jiugao Yu [a], Xiaofei Ma [a,*]

[a] School of Science, Tianjin University, Tianjin 300072, China
[b] Biobased Platforms, Agriculture and Agri-Food Canada, 107 Science Place, Saskatoon, SK, Canada S7N 0X2
[c] Department of Agricultural and Bioresource Engineering, University of Saskatchewan, Saskatoon, SK, Canada S7N 5A9

ARTICLE INFO

Article history:
Received 5 November 2009
Received in revised form 19 November 2009
Accepted 25 November 2009
Available online 3 December 2009

Keywords:
Nanocomposites
Starch
Chitin nanoparticles

ABSTRACT

Contrary to the most recognizable whiskers of slender parallelepiped rods, unique nanoparticles of about 50–100 nm were obtained from chitin after consecutive acid hydrolysis and mechanical ultrasonication treatments. Chitin nanoparticles (CNP) exhibited lower crystallinity when compared to conventional chitin whisker. Glycerol plasticized-potato starch (GPS) was combined with CNP to prepare all-natural nanocomposites by casting and evaporation. The morphology, structural, thermal and mechanical properties of the nanocomposites were evaluated by electron microscopy, X-ray diffraction, dynamic mechanical thermal analysis, and tensile tests. At low loading levels, CNP were uniformly dispersed in the GPS matrix and had good interaction between the filler and matrix, which led to improvements in tensile strength, storage modulus, glass transition temperature, and water vapor barrier properties of the GPS/CNP composites. However, at higher loading (greater than 5 wt.%), aggregation of CNP had a negative effect on these properties.

1. Introduction

Bio-nanocomposites are a new generation of composite materials which have emerged in the frontiers of materials science, life science, and nanotechnology. Most bio-nanocomposites are based on an ingredient fractionated from renewable resources, e.g., cellulose, starch, and proteins (Sorrentino, Gorrasi, & Vittoria, 2007). Because starch is abundant and low cost, it has recently gained much interest as a renewable and biodegradable material for potential products such as water-soluble pouches for detergents and insecticides, flushable liners and bags, and medical delivery devices (Fishman, Coffin, Konstance, & Onwulata, 2000). Native starch commonly exists in a granular structure which can be processed into plasticized starch (PS) in the continuous phase. PS exhibits appropriate physical characteristics, since it is odorless, tasteless, colorless and impermeable to oxygen (Chillo et al., 2008) however, PS shows poor mechanical and moisture barrier properties. One strategy to mitigate the above-mentioned undesirable affect is adding nano-filler (layer silicates, carbon nanotubes, carbon black, and metal oxide nanoparticles) into the PS matrix to form bio-nanocomposites (Chen, Chen, & Evans, 2005; Ma, Chang, & Yu, 2008; Ma, Yu, & Wang, 2008; Yu, Yang, Liu, & Ma, 2009). Recently, much attention has been focused on polysaccharide nano-fillers, such as cellulose nanocrystallites, starch nanocrystals, cellulose esters, and citrate starch nanoparticles, which usually involves several unit operations e.g., acid hydrolysis (Angellier, Molina-Boisseau, Dole, & Dufresne, 2006; Liu & Hu, 2008), dialysis (Hornig & Heinze, 2008) or precipitation (Ma, Jian, Chang, & Yu, 2008).

Chitin is also a biopolymer that is abundant in nature (Wibowo, Velazquez, Savant, & Torres, 2005). It is extracted from crab and shrimp shells as a byproduct of the seafood industry. Under hydrolytic conditions of boiling HCl and vigorous stirring, chitin whiskers of slender parallelepiped rods have been successfully prepared from different chitin sources such as crab shells (Nair & Dufresne, 2003), shrimp shells (Sriupayo, Supaphol, Blackwell, & Rujiravanit, 2005), squid pens (Paillet & Dufresne, 2001), and tubes of *Tevnia jerichonana* (Saito, Putaux, Okano, Gaill, & Chanzy, 1997) and *Riftia pachyptila* tubeworms (Morin & Dufresne, 2002). Noticeably, neither work on the preparation of presumably functional chitin nanoparticles (as opposed to the slender parallelepiped rods), nor its application as a reinforcing filler in polymeric matrices have been reported. We have attempted to make full use of those two renewable and functional ingredients for the preparation of novel biocomposites. We explored the feasibility of bio-nanocomposites composed of all-natural ingredients. In this paper, we report a newly devised procedure for the production of CNP. The thus obtained CNP, which exhibits a more disordered crystal structure than conventional chitin whiskers, was incorporated in a glycerol plasticized-potato starch (GPS) matrix for the development of GPS/CNP bio-nanocomposites. This work focused on processing and characterization of GPS/CNP composites in terms of the morphology, pasting properties, mechanical properties,

* Corresponding authors. Tel.: +86 22 27406144; fax: +86 22 27403475 (X. Ma).
E-mail addresses: peter.chang@agr.gc.ca (P.R. Chang), maxiaofei@tju.edu.cn (X. Ma).

0144-8617/$ - see front matter © 2009 Elsevier Ltd. All rights reserved.
doi:10.1016/j.carbpol.2009.11.041

dynamic mechanical thermal analysis and water vapor permeability.

2. Experimental

2.1. Materials

Potato starch was supplied by Manitoba Starch Products (Manitoba, Canada). Chitin flake from crab leg shells was provided by Panan Chitosan Company Limited, Zhejiang Province, China. Glycerol, hydrochloric acid and sodium hydroxide were purchased from Tianjin Chemical Reagent Factory, China.

2.2. Preparation of chitin nanoparticles (CNP)

Chitin flake (5 g) was initially treated in 3 N hydrochloric acid (400 mL) with vigorous stirring at 105 °C for 3 h; however, the residues after acidic treatment were not immediately dialyzed against distilled water and then lyophilized, as previously described by Nair and Dufresne (2003), for the production of chitin whiskers. Instead, the residue was collected after centrifugation and treated with two identical acidic treatments. Finally, the centrifuged residue was further mechanically disrupted/dispersed in 100 mL distilled water using ultrasonication for 10 min. The suspension was collected and the residue was again disrupted/dispersed in water using ultrasonication. This centrifugation/ultrasonication process was repeated six times in total or until the suspension became clear and the residual precipitate was discarded. The collected suspension was subsequently centrifuged at 12,000g for 20 min. The product was dried and ground to obtain a light yellow CNP powder.

2.3. Processing of GPS/CNP composites

CNP were dispersed in a solution of distilled water (100 ml) and glycerol (1.5 g) and ultrasonicated for 0.5 h before adding 5 g potato starch. The load level of CNP filler (0, 1, 2, 3, 4 or 5 wt.%) was based on the amount of potato starch. The mixture was heated at 90 °C for 0.5 h with constant stirring in order to plasticize the starch, and then cast into a dish and placed in an air-circulating oven at 50 °C until dry (about 6 h). The composites were preconditioned in a climate chamber at 25 °C and 50% RH for at least 48 h prior to testing. Water content of the composites was about 10 wt.%.

2.4. Fourier transform infrared (FTIR) spectroscopy

Chitin and CNP were measured at 2 cm^{-1} resolution with a Bio-Rad FTS 3000 FTIR spectrum scanner.

2.5. X-ray diffractometry

Chitin and CNP powders were tightly packed into the sample holder. X-ray diffraction patterns were recorded in the reflection mode in the angular range of 5°–40° (2θ) at ambient temperature by a BDX 3300 diffractometer, operated at a CuKα wavelength of 1.542 Å. Radiation from the anode, operated at 36 kV and 20 mA, monochromized with a 15 μm nickel foil. The diffractometer was equipped with a 1° divergence slit, 16 mm beam bask, 0.2 mm receiving slit, and a 1° scatter slit. Radiation was detected with a proportional detector.

2.6. Transmission electron microscopy (TEM) and scanning electron microscopy (SEM)

Samples of CNP were prepared from a drop of a dilute suspension deposited and dried on a Formvar grid, and examined using a FEI Tecnai G2 F20. The granular starch and the fracture surfaces of GPS were coated with gold under vacuum, and examined using a Philips XL-3 Scanning Electron Microscope. In order to ascertain dispersion of CNP in the matrix, the fracture surfaces of GPS/CNP composites were tested using a Nanosem 430 Scanning Electron Microscope.

2.7. Rapid visco analyser (RVA)

Pasting properties were measured on a Rapid Visco Analyser (Newport Scientific, Sydney, Australia) according to AACC method 76-21 (Xie & Liu, 2004). CNP particles were dispersed in a solution of distilled water (25 ml) and glycerol (0.375 g) using ultrasonication for 0.5 h before 1.25 g potato starch was added. The obtained starch slurry had the same composition as the GPS/CNP composite mixture before casting. The starch slurry was kept at 50 °C for 1 min, heated to 95 °C at 12.2 °C/min and held at 95 °C for 2.5 min. It was then cooled to 50 °C (cooling rate of 11.8 °C/min) and held at 50 °C for 2 min. The paddle speed was 960 rpm for 10 s and then decreased to 160 rpm for the rest of the experiment.

2.8. Mechanical testing

The Testometric AX M350-10KN Materials Testing Machine was operated with a crosshead speed of 50 mm/min for tensile testing (ISO 1184-1983 standard). The result was the average of 5–8 specimens.

2.9. Dynamic mechanical thermal analysis (DMTA)

The GPS/CNP composites were tested using a Netzsch DMA 242 analyzer operating at 1 Hz frequency. DMTA scans were performed between −80 and 80 °C with a heating rate of 3 °C/min.

2.10. Water vapor permeability (WVP)

WVP tests were carried out using ASTM method E96 (1996) with some modifications (Yu, Wang, & Ma, 2008). RH 0% was maintained using anhydrous calcium chloride in the cell. The composites were cut into circles and the cell sealed over with melted paraffin. Each cell was stored in a desiccator containing water to provide a constant RH of 100% at 25 °C. WVP was determined by calculating the weight gain of the permeation cell. Changes in the weight of the cell were recorded as a function of time. Slopes were calculated by linear regression (weight change vs. time) and correlation coefficients for all reported data were >0.99. The water vapor transmission rate (WVTR) was defined as the slope (g/s) divided by the transfer area (m^2). After the permeation tests, film thickness was measured and WVP (g $Pa^{-1}s^{-1}m^{-1}$) was calculated as:

$$WVP = \frac{WVTR}{P(R_1 - R_2)} \cdot x$$

where P is the saturation vapor pressure of water (Pa) at the test temperature (25 °C), R_1 is the RH in the desiccator, R_2 is the RH in the permeation cell, and x is the film thickness (m). Under these conditions, the driving force $P(R_1 - R_2)$ is 2338 Pa.

3. Results and discussion

3.1. Characterization of CNP

In the FTIR spectra of chitin and CNP (Fig. 1(a)), broad peaks at 3430 and 3258 cm^{-1} were ascribed to the O–H and N–H stretch vibrations, respectively (Hu et al., 2007). The FTIR spectrum of CNP (Fig. 1) confirmed the existence of α-chitin with convincing

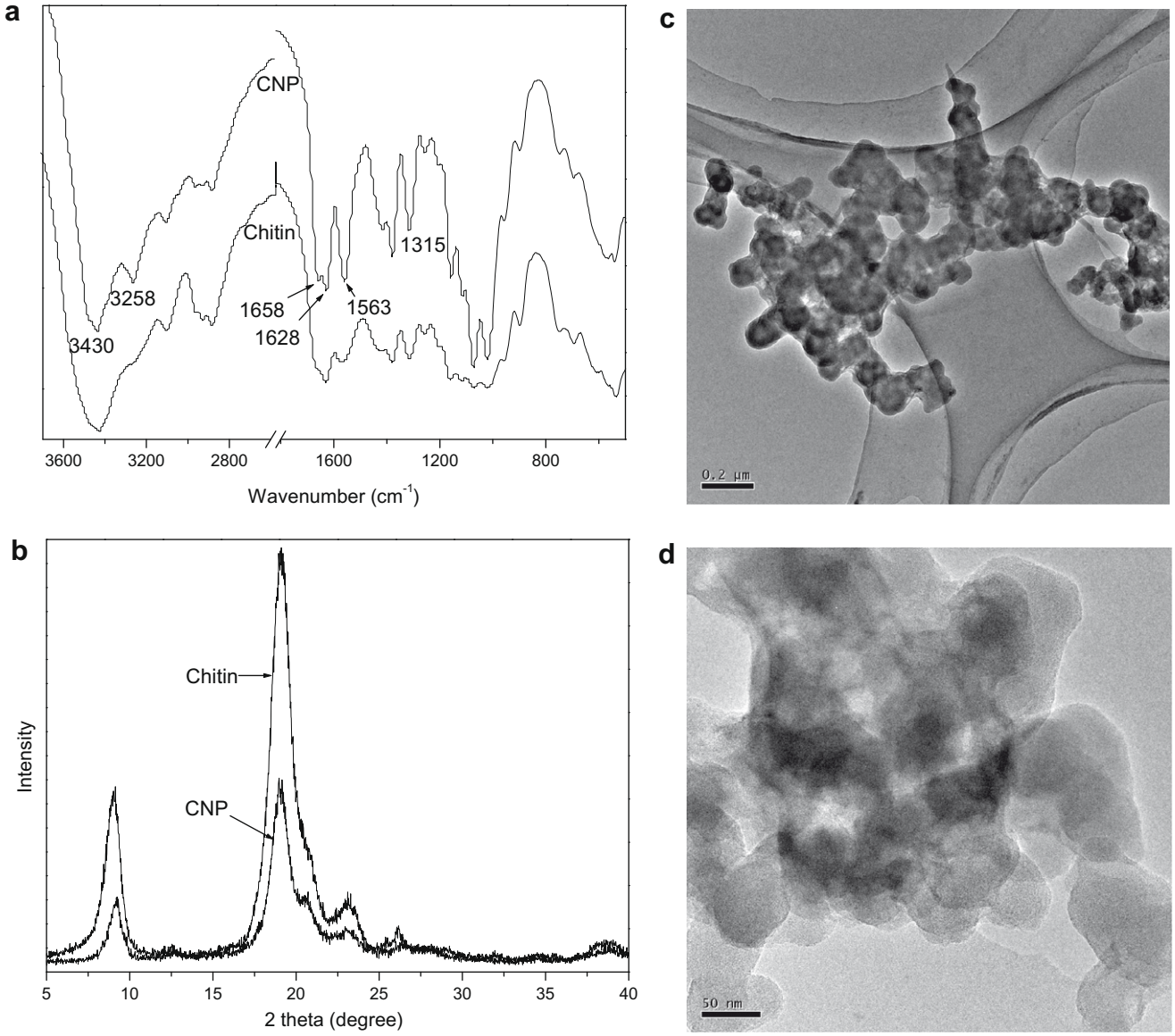

Fig. 1. Characterization of CNP. (a) FTIR spectrum of chitin and CNP; (b) X-ray diffractograms of chitin and CNP; (c) and (d) TEM of CNP.

characteristic peaks at 1658 and 1628 cm^{-1} for amide I, 1563 cm^{-1} for amide II, and 1315 cm^{-1} for amide III (Nair & Dufresne, 2003; Phongying, Aiba, & Chirachanchai, 2007). The absorption bands between 1000 and 1200 cm^{-1} were characteristic of –C–O– stretching of a polysaccharide skeleton (Wang, Chen, Zhang, & Yu, 2008). CNP exhibited sharper characteristic peaks and splitting of the C=O stretching band (amide I) as compared to the chitin flake. This indicated that the HCl solution may have changed the structure of chitin (Hu et al., 2007) and the hydrogen bonding interaction in CNP. According to Sikorski, Hori, and Wada (2009) it is possible that disordered crystal structure plays a role in the splitting of the amide I band of α-chitin.

The XRD patterns (Fig. 1(b)) of chitin and CNP showed sharp crystalline reflections at about 9.2°, 19.1°, 23.2° and 26.1°, consistent with reported values for α-chitin (Al-Sagheer, Al-Sughayer, Muslim, & Elsabee, 2009). The crystallinity of CNP obviously decreased as compared to the chitin which is consistent with the FTIR results. Although acid hydrolysis was faster in the amorphous region than in the crystalline region of chitin, both amorphous and crystalline regions were attacked when chitin was treated with hydrochloric acid. During CNP processing, some parts of crystallite were converted to amorphous chitin while the amorphous region was unchanged. Consequently, the crystallinity of CNP is lower than that of native chitin.

Chitin whiskers, composed mainly of slender parallelepiped rods, are usually prepared by treating chitin with hydrochloric acid, followed by dialyzing the residues in distilled water until neutral, and then lyophilizing (Nair & Dufresne, 2003). With consecutive implementation of acidic hydrolysis and mechanical ultrasonication/disruption, chitin nanoparticles of about 50–100 nm were formed rather than chitin whiskers, as evidenced in Fig. 1(c) and (d). It is quite apparent that the amorphous chitin is further removed from chitin during the preparation of chitin whisker, resulting in higher crystallinity in chitin whiskers as compared to native chitin. On the other hand, opposite to what happens during the preparation of chitin whisker, in CNP some crystalline portions are removed which resulting in lower crystallinity as shown in Fig. 1(b).

3.2. Morphology of GPS/CNP composites

As compared to native potato starch granules (Fig. 2(a)) which are 10–50 μm, no residual granular structure is present in the con-

tinuous GPS phase (Fig. 2(b)). At high temperature, water and glycerol are known to physically break up starch granules and disrupt intermolecular and intramolecular hydrogen bonds resulting in plastic native starch (Yu et al., 2009).

The morphology of composites is a very important characteristic in determining many properties of composite films. The distribution of CNP in the GPS matrix is shown in Fig. 2(c) and (d). At low CNP concentration (2 wt.%), most CNP are dispersed uniformly in the GPS matrix without obvious aggregation (Fig. 2(c)), which is ascribed to strong interaction because of the similar polysaccharide structures of CNP and potato starch in the GPS matrix. However, at a high filler content (5 wt.%) conglomeration of CNP was obvious (Fig. 2(d)).

3.3. RVA

The rapid visco analyser (RVA) is an effective instrument for determining the pasting properties of starch. The effect of CNP content on pasting curves of potato starch slurry was tested during a heating–cooling cycle, which is shown in the temperature pattern of Fig. 3. To simulate the composite making process, the potato starch slurry had the same composition as the GPS/CNP mixtures. The pasting profiles of the starch slurries with different CNP concentrations are similar. When granular starch began to plasticize and dissolve in water, the starch slurry turned into a starch solution, and the viscosity increased. When CNP was added, the peak viscosity of the starch slurry obviously decreased and shifted to a lower temperature. This means that the addition of CNP is propitious to the plasticization of starch and to a decrease in the interaction between starch molecules. The higher the CNP content, the higher the pasting curves were. The pasting viscosity increased with the increasing CNP content. The interaction between CNP and starch was presumably increased, as such a small amount of CNP (about 0.05 wt.% of starch solution) resulted in a profound increase in viscosity.

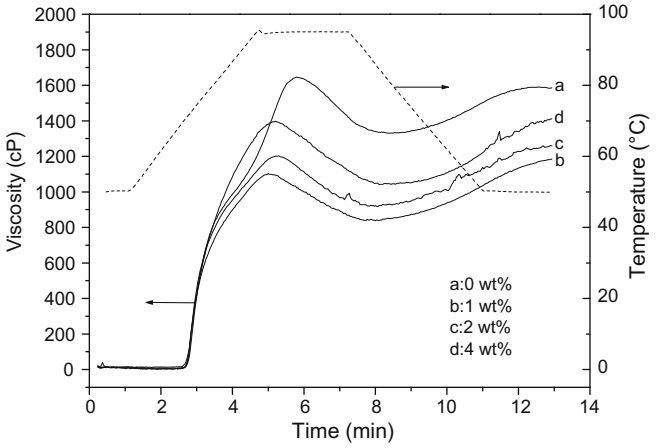

Fig. 3. Effect of CNP content on the pasting profile.

3.4. Mechanical testing

Fig. 4 exhibits the effect of CNP content on the mechanical properties of GPS/CNP composites. As the filler in GPS matrix, CNP had an obvious reinforcing effect. When the CNP content varied from 0 to 5 wt.%, the tensile strength increased from 2.84 to 7.79 MPa, but the elongation at break decreased from 59.3% to 19.3%. This can be ascribed to good interfacial interaction between CNP and GPS matrix because of the similar polysaccharide structures of chitin and starch.

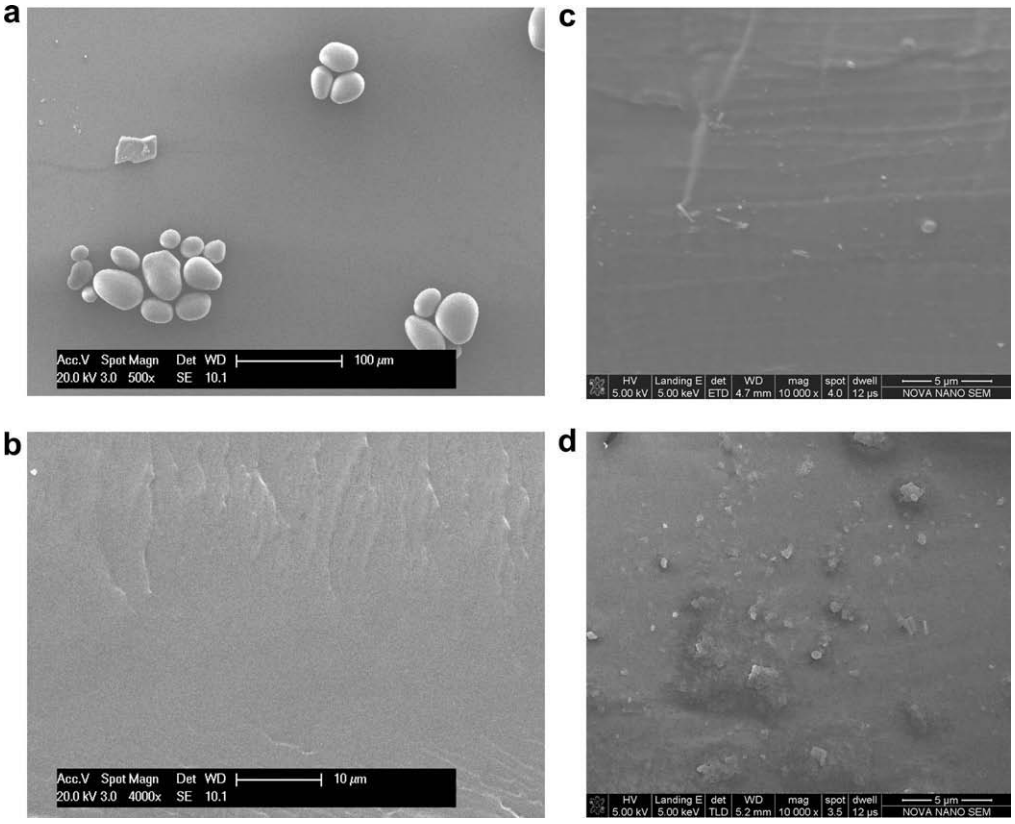

Fig. 2. SEM micrographs of native potato starch (a), the fragile fractured surface of GPS (b), and GPS/CNP composites containing 2 wt.% CNP (c) and 5 wt.% CNP (d).

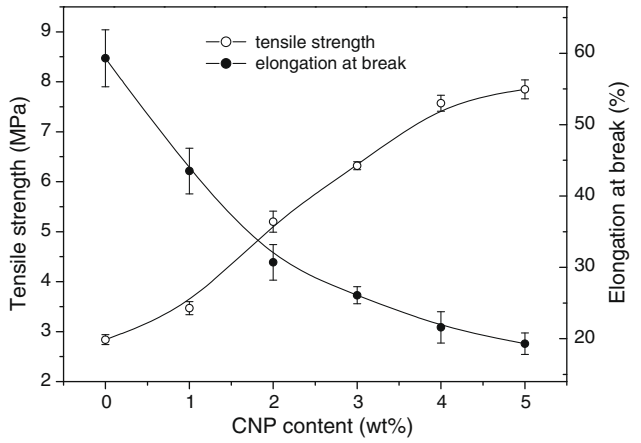

Fig. 4. Effect of CNP content on tensile strength and elongation at break of GPS/CNP composites.

3.5. DMTA

Fig. 5(a) shows the effect of CNP concentration on the storage modulus as a function of temperature for GPS/CNP composites. The storage modulus, detected by DMTA, relates to composite stiffness. When CNP was introduced, the storage modulus of GPS/CNP composites increased. Fig. 5(b) shows the curves for loss factor (tan delta) as a function of temperature for GPS/CNP composites. In the region corresponding to the maximum loss factor (tan delta), the decrease in storage modulus was usually rapid. The loss factor is sensitive to molecular motion and its peak represents the glass transition temperature. The curve of GPS revealed two thermal transitions corresponding to the two separate phases in GPS (Ma, Chang, Yu, & Stumborg, 2009). The upper transition (19.6 °C), due to a starch-rich phase, is regarded as the glass transition temperature (T_g) of GPS, while the lower transition (−57.2 °C) was due to a starch-poor phase. In GPS/CNP composites, both the upper transition and the lower transition shifted to higher temperatures, which indicated that both the starch-rich and starch-poor phases interacted well with CNP. Serving as junctions, CNP improved the intermolecular interaction of GPS in the starch-rich phase, bringing adjacent chains of starch close, restraining chain mobility, and reducing the free volume (Yu et al., 2008); thereby raising the T_g of composites as the CNP content increased. It was also noted that a double-peak of loss factor appeared at 31.6 and 46.4 °C for GPS/CNP composites with a CNP content of 5 wt.%, in which CNP aggregation was obvious, as shown in Fig. 2(d). Aggregation of CNP would result in the heterogeneous collection of GPS matrix and CNP filler. The higher transition temperature (46.4 °C) may have been due to a CNP-rich phase, while the lower transition (31.6 °C) to a CNP-poor phase.

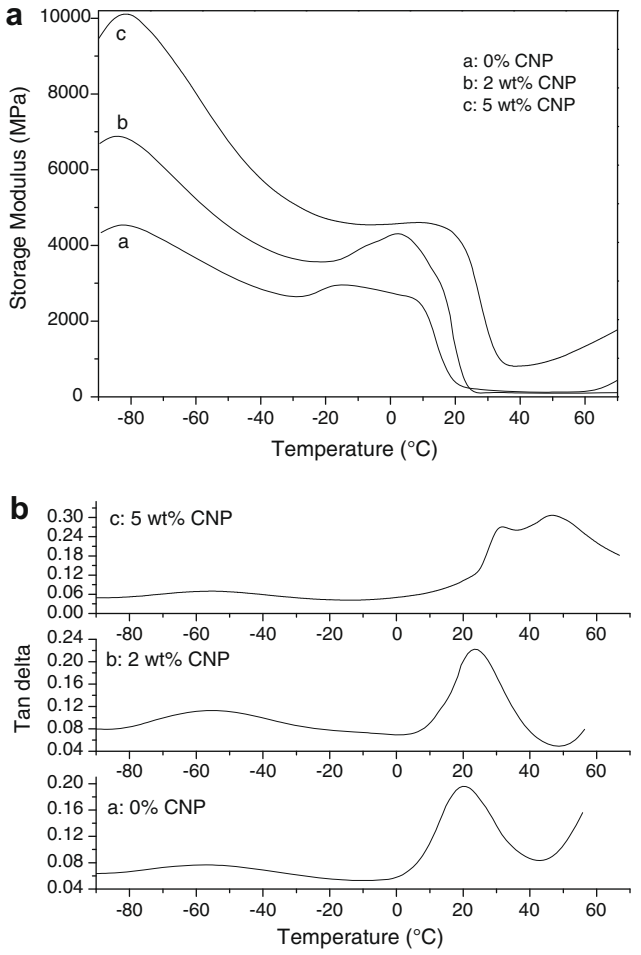

Fig. 5. Storage modulus (a) and tan delta (b) of GPS/CNP composites with different CNP contents.

3.6. WVP of the composites

Water vapor permeability (WVP) is often used to study moisture transport through a film. As shown in Fig. 6, WVP of GPS/CNP composites decreased with increasing CNP concentration. WVP of GPS reached a peak value of 5.62×10^{-10} g m^{-1} s^{-1} Pa^{-1}. WVP values obviously decreased when the CNP content increased from 1 to 3 wt.%, and then decreased only slightly when the CNP content increased from 3 to 5 wt.%, i.e. 3.45×10^{-10} g m^{-1} s^{-1} Pa^{-1} at 3 wt.% and 3.41×10^{-10} g m^{-1} s^{-1} Pa^{-1} at 5 wt.%. The water resistance of CNP was better than that of the GPS matrix; however, the addition of CNP introduced a tortuous path for water molecules to pass through the composites (Yu et al., 2009). CNP dispersed well in the matrix at low CNP concentrations and so there were fewer paths for water molecules to pass through the composites; however, superfluous CNP aggregated (as shown by Fig. 2(d)), which contrarily facilitated water vapor permeation.

4. Conclusion

As a novel product of the acid hydrolysis of chitin, CNP exists in α-chitin with more less-ordered domains than native chitin. When CNP was added at low loading levels, it dispersed uniformly in the

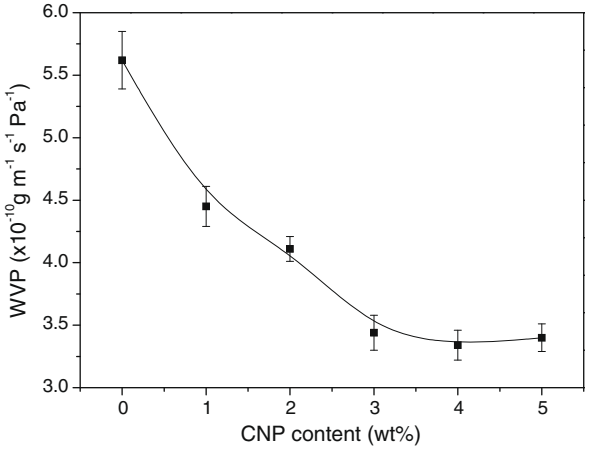

Fig. 6. Effect of CNP content on water vapor permeability of GPS/CNP composites.

GPS matrix, and the tensile strength, storage modulus, glass transition temperature, and water vapor permeability of GPS/CNP composites improved because of good interfacial interaction between CNP filler and GPS matrix. However, the elongation at break of the GPS/CNP composites decreased. These natural polysaccharide bio-nanocomposites have potential applications in medical, agricultural, pharmaceutical and packaging fields as edible films, food packaging and one-off packaging.

References

Al-Sagheer, F. A., Al-Sughayer, M. A., Muslim, S., & Elsabee, M. Z. (2009). Extraction and characterization of chitin and chitosan from marine sources in Arabian Gulf. *Carbohydrate Polymers, 77*, 410–419.

Angellier, H., Molina-Boisseau, S., Dole, P., & Dufresne, A. (2006). Thermoplastic starch-waxy maize starch nanocrystals nanocomposites. *Biomacromolecules, 7*, 531–539.

Chen, M., Chen, B. Q., & Evans, J. R. G. (2005). Novel thermoplastic starch-clay nanocomposite foams. *Nanotechnology, 16*, 2334–2337.

Chillo, S., Flores, S., Mastromatteo, M., Conte, A., Gerschenson, L., & Del Nobile, M. A. (2008). Influence of glycerol and chitosan on tapioca starch-based edible film properties. *Journal of Food Engineering, 88*, 159–168.

Fishman, M. L., Coffin, D. R., Konstance, R. P., & Onwulata, C. I. (2000). Extrusion of pectin/starch blends plasticized with glycerol. *Carbohydrate Polymers, 41*, 317–325.

Hornig, S., & Heinze, T. (2008). Efficient approach to design stable water-dispersible nanoparticles of hydrophobic cellulose esters. *Biomacromolecules, 9*, 1487–1492.

Hu, X. W., Du, Y. M., Tang, Y. F., Wang, Q., Feng, T. Yang, & Kennedy, J. F. (2007). Solubility and property of chitin in NaOH/urea aqueous solution. *Carbohydrate Polymers, 70*, 451–458.

Liu, Y. P., & Hu, H. (2008). X-ray diffraction study of bamboo fibers treated with NaOH. *Fibers and Polymers, 9*, 735–739.

Ma, X. F., Chang, P. R., & Yu, J. G. (2008). Characterizations of glycerol plasticized-starch (GPS)/carbon black (CB) membranes prepared by melt extrusion and microwave radiation. *Carbohydrate Polymers, 74*, 895–900.

Ma, X. F., Chang, P. R., Yu, J. G., & Stumborg, M. (2009). Properties of biodegradable citric acid-modified granular starch/thermoplastic pea starch composites. *Carbohydrate Polymers, 75*, 1–8.

Ma, X. F., Jian, R. J., Chang, P. R., & Yu, J. G. (2008). Fabrication and characterization of citric acid-modified starch nanoparticles/plasticized-starch composites. *Biomacromolecules, 9*, 3314–3320.

Ma, X. F., Yu, J. G., & Wang, N. (2008). Glycerol plasticized-starch/multiwall carbon nanotube composites for electroactive polymers. *Composites Science and Technology, 68*, 268–273.

Morin, A., & Dufresne, A. (2002). Nanocomposites of chitin whiskers from Riftia tubes and Poly(caprolactone). *Macromolecules, 35*, 2190–2199.

Nair, K. G., & Dufresne, A. (2003). Crab shell chitin whisker reinforced natural rubber nanocomposites. 1. Processing and swelling behavior. *Biomacromolecules, 4*, 657–665.

Paillet, M., & Dufresne, A. (2001). Chitin whisker reinforced thermoplastic nanocomposites. *Macromolecuels, 34*, 6527–6530.

Phongying, S., Aiba, S., & Chirachanchai, S. (2007). Direct chitosan nanoscaffold formation via chitin whiskers. *Polymer, 48*, 393–400.

Saito, Y., Putaux, J. L., Okano, T., Gaill, F., & Chanzy, H. (1997). Structural aspects of the swelling of β chitin in HCl and its conversion into α chitin. *Macromolecules, 30*, 3867–3873.

Sikorski, P., Hori, R., & Wada, M. (2009). Revisit of α-chitin crystal structure using high resolution X-ray diffraction data. *Biomacromolecules, 10*, 1100–1105.

Sorrentino, A., Gorrasi, G., & Vittoria, V. (2007). Potential perspectives of bio-nanocomposites for food packaging applications. *Trends in Food Science and Technology, 18*, 84–95.

Sriupayo, J., Supaphol, P., Blackwell, J., & Rujiravanit, R. (2005). Preparation and characterization of α-chitin whisker-reinforced chitosan nanocomposite films with or without heat treatment. *Carbohydrate Polymers, 62*, 130–136.

Wang, J. P., Chen, Y. Z., Zhang, S. J., & Yu, H. Q. (2008). A chitosan-based flocculant prepared with gamma-irradiation-induced grafting. *Bioresource Technology, 99*, 3397–3402.

Wibowo, S., Velazquez, G., Savant, V., & Torres, J. A. (2005). Surimi wash water treatment for protein recovery: effect of chitosan–alginate complex concentration and treatment time on protein adsorption. *Bioresource Technology, 96*, 665–671.

Xie, X. J., & Liu, Q. (2004). Development and physicochemical characterization of new resistant citrate starch from different corn starches. *Starch/Starke, 56*, 364–370.

Yu, J. G., Wang, N., & Ma, X. F. (2008). Fabrication and characterization of poly(lactic acid)/acetyl tributyl citrate/carbon black as conductive polymer composites. *Biomacromolecules, 9*, 1050–1057.

Yu, J. G., Yang, J. W., Liu, B. X., & Ma, X. F. (2009). Preparation and characterization of glycerol plasticized-pea starch/ZnO-carboxymethylcellulose sodium nanocomposites. *Bioresource Technology, 100*, 2832–2841.